KeAi
CHINESE ROOTS
GLOBAL IMPACT

Contents lists available at ScienceDirect

Petroleum Science

journal homepage: www.keaipublishing.com/en/journals/petroleum-science



Original Paper

Experimental study of acid fracturing behavior in carbonate reservoirs with different fracture-cavity development



Song-Cai Han $^{\rm a}$, Li-Le Li $^{\rm a}$, Sen Hu $^{\rm a}$, Chu-Hao Jing $^{\rm a}$, Xu-Di Wu $^{\rm a}$, Jun-Chao Yang $^{\rm c}$, Tao Liu $^{\rm a,\,d,\,*}$, Cai-Yun Xiao $^{\rm b,\,**}$

- ^a College of Energy, Chengdu University of Technology, Chengdu, 610059, Sichuan, China
- ^b School of Resources and Safety Engineering, Chongqing University, Chongqing, 400044, China
- ^c School of Petroleum Engineering, China University of Petroleum (East China), Qingdao, 266580, Shandong, China
- d Tight Oil & Gas Exploration and Development Department, PetroChina Southwest Oil & Gasfield, Chengdu, 610051, Sichuan, China

ARTICLE INFO

Article history: Received 28 November 2024 Received in revised form 22 April 2025 Accepted 22 April 2025 Available online 29 April 2025

Edited by Yan-Hua Sun

Keywords:
Carbonate formations
Acid fracturing
Fracture-cavity development
Alternating injection
Fracture morphology

ABSTRACT

Heterogeneity in carbonate formations due to discontinuities (e.g., fractures and cavities) will bring about distinctive acid stimulation effects. However, the differences in fracturing behavior between homogeneous and heterogeneous carbonate formations remain unclear, complicating the optimization of acid fracturing strategies. In this paper, full-diameter carbonate rock samples with different degrees of discontinuity development are selected to investigate the fracturing behavior under different fluid types and injection schemes. Advanced techniques, including 3D CT scanning and 3D laser scanning, are employed to analyze fracture morphology and etching characteristics, respectively. Experimental results show that the coupled hydraulic-chemical effects play different roles in fracture induction between fracture-cavity developed and undeveloped carbonate rocks. Acid-fracturing stimulation consistently induces multiple types of complex fractures in fracture-cavity carbonate rocks, whereas it results in a single artificial fracture in less fracture-cavity carbonate rocks. Furthermore, localized etching patterns are prevalent in most fracture-cavity carbonate rocks, whereas homogeneous carbonate rocks exhibit regional or global etching characteristics. In both carbonate rocks, the stimulation effect of guar fluid is inferior to that of gelled acid but comparable to self-generating acid. Further findings are that alternating fracturing with guar and acid fluids in fracture-cavity carbonate rocks can sustain or even increase the injection pressure, facilitating the formation of new or depth-penetrating fractures. This phenomenon, however, is not observed in fracture-cavity undeveloped carbonate rocks. Potential interaction modes between induced fracture and natural fractures/cavities under different injection conditions are also identified. Finally, preferred fracturing schemes applicable to different carbonate formations are recommended based on the area, number and roughness of the induced fractures.

© 2025 The Authors. Publishing services by Elsevier B.V. on behalf of KeAi Communications Co. Ltd. This is an open access article under the CC BY-NC-ND license (http://creativecommons.org/licenses/by-nc-nd/4.0/).

1. Introduction

Carbonate reservoirs are one of the most important unconventional oil and gas reservoirs, whose reserve accounts for approximately 70% of the global oil and gas resources ascertained worldwide (Li et al., 2018). In the light of the low porosity and

Peer review under the responsibility of China University of Petroleum (Beijing).

permeability of deep carbonate formations, permeability enhancement technologies are essential for the high-efficient development of carbonate reservoirs. In contrast to shale reservoir stimulation, acid treatment-induced etching fractures are the most widely used method to improve the conductivity of carbonate formations (Aljawad et al., 2019). However, in carbonate formations a large number of natural fractures, joints, cavities (or vugs), and dissolution pores are developed, which will result in notable heterogeneity and complexity in hydraulic-mechanical properties. Fracture propagation modes induced by high-pressure acid fluids are absolutely different in fracture-cavity developed and undeveloped carbonate reservoirs (Liu et al., 2020; Qiao et al., 2022; Zhu

st Corresponding author.

^{**} Corresponding author.

E-mail addresses: liutao.xn@petrochina.com.cn (T. Liu), xiaocy@cqu.edu.cn (C-Y. Xiao).

et al., 2023). At present, it is still unclear about the fracturing behavior of carbonate formations with different degrees of fracture-cavity development under the pressure-coupled-dissolution effect, which severely restricts the optimization of acid fracturing schemes.

Discontinuous structures (e.g., fractures and cavities) within carbonate reservoirs have a significant effect on the fracture propagation behavior and the induced fracture morphology. At present, extensive experimental and numerical investigations have examined the interaction between hydraulic fractures and natural fractures or cavities (Cheng et al., 2014; Huang et al., 2019; Han et al., 2020; Kao et al., 2022; Qiao et al., 2022; Suo et al., 2024; Yang et al., 2024). Generally, five propagation scenarios may be identified when a hydraulic fracture encounters natural fractures or cavities, namely crossing, blocking, deflecting, bypassing or multiple-cases appearing. Regrettably, the chemical dissolutioninduced etching process is not involved in these studies. Some researchers have resorted to numerical simulations to investigate the propagation behavior of acid-etched wormholes or acid-induced fractures in fracture-cavity carbonate rocks (Liu et al., 2017; Chen et al., 2018; Luo et al., 2020; Xu et al., 2021; Zhu et al., 2023). However, experimental studies of acid-induced fracturing behavior in carbonate reservoirs are relatively rare, especially with respect to the degree of development of fractures and cavities. Hou et al. (2019) and Zhang et al. (2020) experimentally investigated for the first time the effect of natural fractures on the propagation behavior of acid-induced fractures in carbonate outcrops. However, the development degree and distribution characteristics of natural fractures and cavities are not considered, leaving uncertainty about the differences in fracturing behavior between fracture-cavity developed and undeveloped carbonate formations.

In fracture-cavity developed carbonate reservoirs, a thorny issue associated with acid fracturing is the leakage of the acid fluid, which will reduce the effectiveness of acid penetration distance. Generally, successful acid fracturing treatment requires not only high fracture conductivity, but also a long acid penetration distance (Oeth et al., 2013; Hou et al., 2019; Zhao et al., 2020). It is imperative to address which fracturing scheme is preferable for a given carbonate formation to achieve a better stimulation performance. Currently, some special treatments have been designed to alleviate the issue, such as increasing the viscosity of acid (Zhou et al., 2007; Gao et al., 2019; Wang et al., 2024), adopting multi-stage alternating acid fracturing (Mou and Zhang, 2015; Gou et al., 2021; Wang et al., 2022; Zhang et al., 2020; Zhao et al., 2022) or applying diverting acid as a temporary plugging agent (Zhao et al., 2020; Mahdaviara et al., 2021; Al-Shargabi et al., 2023). Among them, onspot practices have confirmed that fracturing with alternating injection of fracturing fluids and acid fluids is an effective method to reduce the leakage of acid fluid. Some experiments have also been conducted to investigate the fracturing behavior and etching characteristics during alternating injections, including fracturing fluids alternating with gelled acid, cross-linked acid or selfgenerating acid, self-generating acid alternating with gelled acid or cross-linked acid, and fracturing fluids alternating with selfgenerating acid + cross-linked acid or gelled acid (Kao et al., 2019; Zhang et al., 2020; Zhao et al., 2022; Liu et al., 2024). However, the fracture propagation behavior and the interaction mechanisms between induced fractures and natural fractures/cavities during alternating acid fracturing are still ambiguous. The feasibility of using multi-stage alternating injection fracturing to achieve a better stimulation effect also needs further experimental confirmation.

In this paper, two types of carbonate reservoirs with different fracture-cavity development are used to uncover the fracturing behavior under different fluid types (including guar fluid, gelled acid, and self-generating acid) and injection schemes (single injection and alternating injection). Meanwhile, the interaction between hydraulic fractures and natural discontinuities is analyzed. A comparative analysis of the stimulation effect of the two types of rocks is elaborated, and a preference of the acid fracturing scheme is also recommended. The research results can provide some theoretical support for the design of acid fracturing in carbonate formations.

2. Methodology

2.1. Specimen preparation

Full-diameter carbonate rock samples were collected from the Permian Maokou Formation at a depth of 4257–4340 m in the southeastern Sichuan Basin, China. The X-ray diffraction measurement shows that the rock minerals consist of 78% dolomite, 12% calcite, 7.8% quartz + feldspar, and 2.2% clay in average. The rock mechanics tests show that the carbonate rock has an average tensile strength of 7.1 MPa, an average uniaxial compressive strength of 60.8 MPa, and an average I-type fracture toughness of 0.64 MPa $\,\mathrm{m}^{0.5}$. The samples were then cut into standard cylinders with a length of 110 mm and a diameter of 100 mm through a wirecutting machine (Fig. 1(a)). In order to exert true triaxial stress conditions, all standard cylinders were enclosed with cement to form a cube with dimensions of 110 mm \times 110 cm \times 110 cm, as shown in Fig. 1(b). Subsequently, an open hole with a diameter of 8 mm and a length of 55 mm was then drilled along the axial direction of the specimen. The upper portion of the open hole with a length of 20 mm was enlarged with a 10 mm drill bit to accommodate the seal tube, as shown in Fig. 1(c).

2.2. Experimental design

Considering the heterogeneity of the carbonate rocks, all standard specimens were first scanned using high-energy computed tomography (CT) to quantify the number of natural fractures and cavities (or vugs). According to the degree of development of fractures and cavities, 10 specimens are categorized into two types: (i) fracture-cavity developed carbonate rocks, in which the number of both fractures and cavities is generally greater than 2, or some fractures are close to or connected to the wellbore; and (ii) fracture-cavity undeveloped carbonate rocks, in which the number of fractures or cavities is less than 2, and the natural fractures and cavities are away from the wellbore, as shown in Fig. 2. For these two types of carbonate rocks, different fracturing schemes are purposely designed to uncover fluid injection-induced fracturing characteristics, including fracture initiation and propagation, fracture etching degree, and final fracture morphology.

The Permian Maokou Formation with a depth of 4257–4340 m is subjected to a maximum horizontal stress with 120.5–127.9 MPa, a vertical stress with 109.7-121.0 MPa and a minimum horizontal stress with 100.6-107.7 MPa. The in-situ stress regime with such large horizontal stress differences (15.4-23.3 MPa) generally generates relatively simple vertical fractures during fracturing. Based on the second similarity theory (Liu et al., 2000; Sarmadivaleh and Rasouli, 2015), all experiments are designed with a pump rate of 5 mL/min and a horizontal stress difference of 15 MPa. It is noteworthy that the pump rate in all experiments is relatively low so that there is sufficient time for the injection of the subsequent fluid and the full reaction between carbonate rocks and acid fluids. The final fracturing schemes for carbonate formations with different degrees of fracture-cavity development are generalized in Table 1. In this study, four fracturing fluids including guar fluid, gelled acid, self-generating acid, and diverting acid are selected to investigate

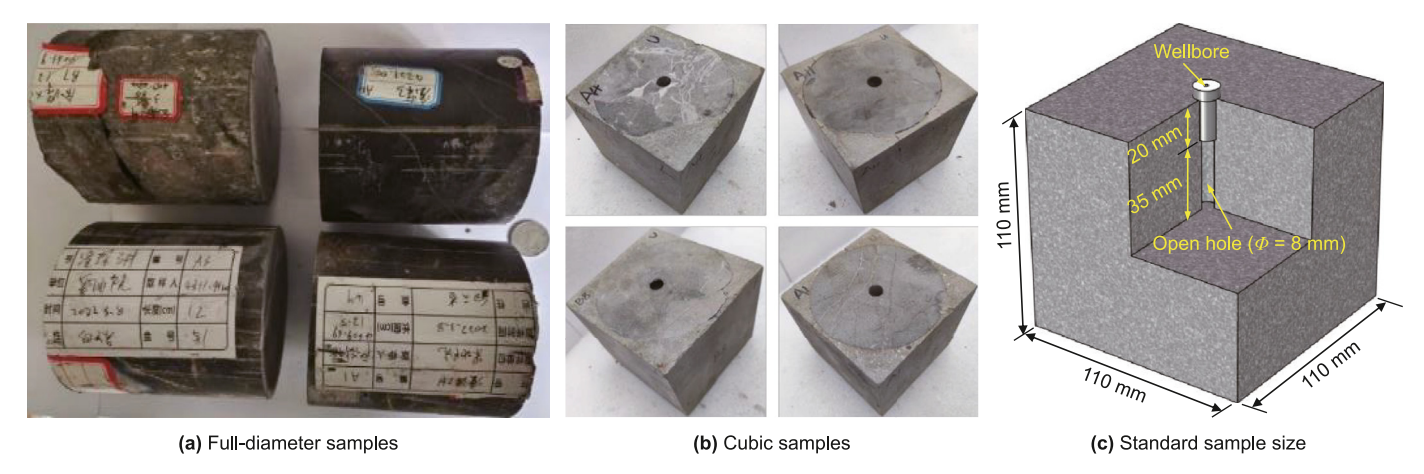


Fig. 1. The preparation process of experimental specimens.

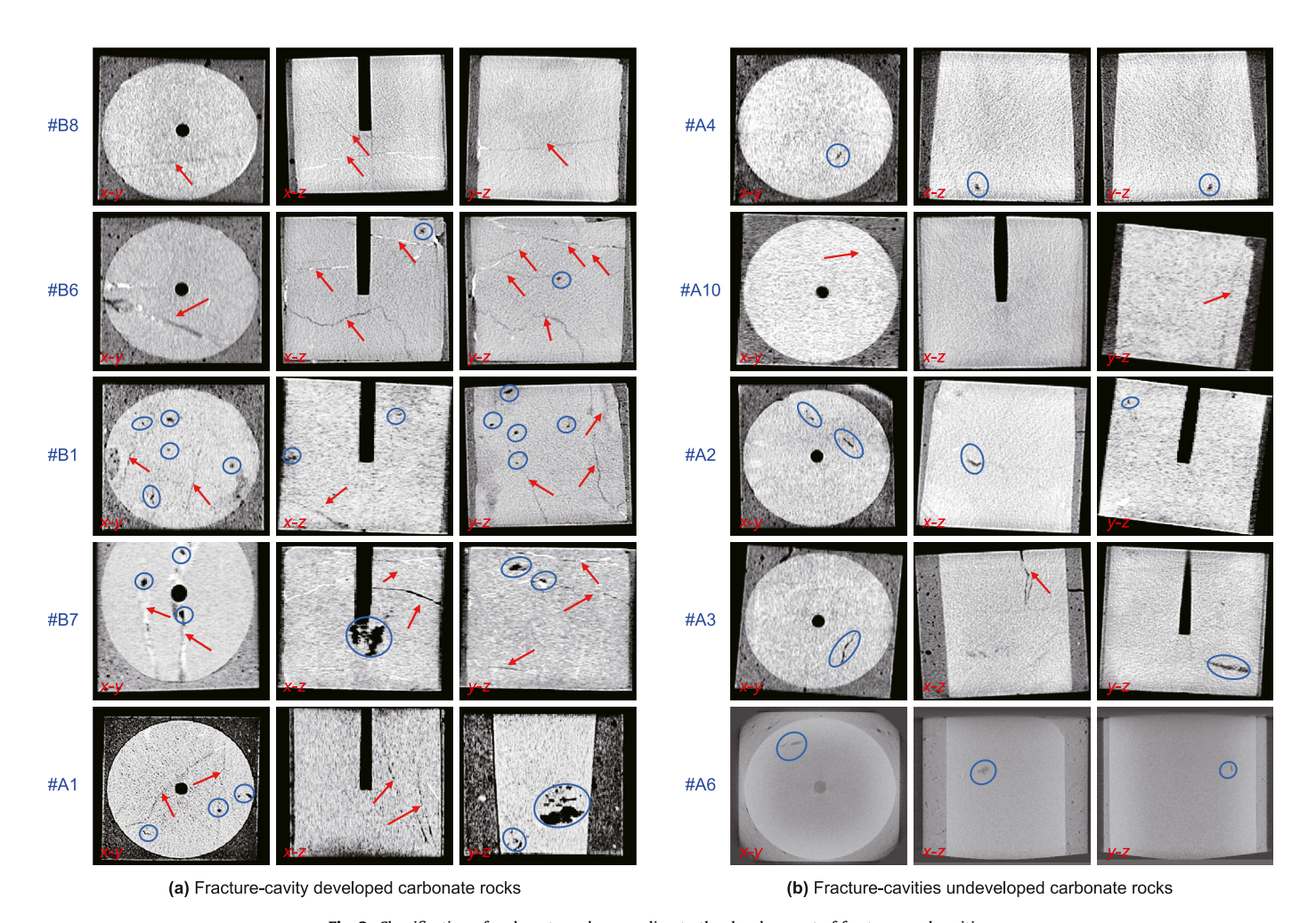


Fig. 2. Classification of carbonate rocks according to the development of fractures and cavities.

fluid injection-induced fracturing behavior. Self-generating acid has a lower reaction rate than gelled acid at room temperature, so it is also used as pad fluid to cool formations and create artificial fractures. The viscosity of the diverting acid will increase obviously as the acid—rock reaction proceeds, so it is used as the temporary plugging agent to seal these highly conductive fractures.

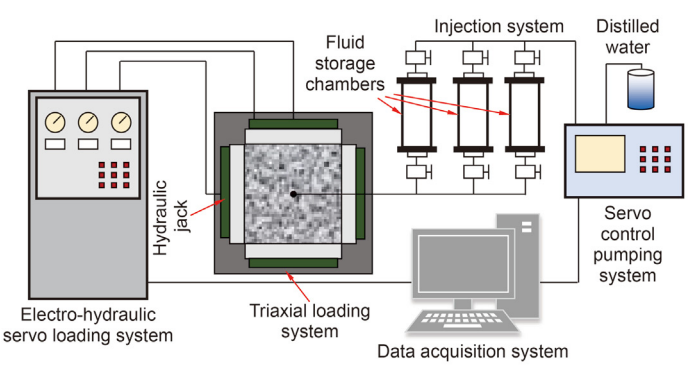
2.3. Experimental apparatus

The self-developed experimental system consists of a true triaxial loading system, a fluid injection system, two servo control systems, and a data acquisition system, as shown in Fig. 3. The triaxial loading system, the fluid injection system as well as the pipelines and valves are specially designed with acid-proof

Table 1 Fracturing scheme designs for different carbonate rocks.

Label	Number of fractures and cavities based on CT scanning	Rock type	Vertical stress, MPa	Maximum horizontal stress, MPa	Minimum horizontal stress, MPa	Pump rate, mL/min		Number of alternating stages
#B8	3/0	Fracture-cavity	30	35	20	5	Guar fluid	_
#B6	3/2	developed carbonate	30	35	20	5	Gelled acid	_
#B1	2/8	rock	30	35	20	5	Guar fluid + gelled acid	1
#B7	3/4		30	35	20	5	Self-generating acid + gelled acid	1
#A1	4/5		30	35	20	5	$Guar\ fluid + gelled\ acid$	2
#A4	0/1	Fracture-cavity	30	35	20	5	Guar fluid	_
#A10	1/0	undeveloped carbonate	30	35	20	5	Gelled acid	_
#A2	0/4	rock	30	35	20	5	Guar fluid + gelled acid	1
#A3	1/3		30	35	20	5	Self-generating acid + gelled acid	1
#A6	0/3		30	35	20	5	Guar fluid + gelled acid + diverting acid	2

Note: Guar fluid consists of 0.4% guar powder +0.2% crosslinker +0.5% clay stabilizer; gelled acid consists of 20% HCl +0.8% gelled agent +3% corrosion inhibitor +1% ferric ion stabilizer +0.3% clay stabilizer; the ingredients of self-generating acid and diverting acid are confidential in this study.





(a) Schematic of the experimental apparatus

(b) Picture of the experimental apparatus

Fig. 3. Experimental apparatus for acid fracturing.

Hastelloy metal to avoid acid corrosion. The injection system contains three storage chambers that can be used to simulate the alternating fracturing process with different fluids. The true triaxial test system can accommodate rock specimens with a maximum size of 110 mm \times 110 mm \times 110 mm. The in-situ stresses are applied by three pairs of hydraulic jacks which are driven by silicon oil booster pumps with a maximum output pressure of 50 MPa. The fracturing fluids in the storage chambers are pumped by plunger pumps which are driven by the servo booster through distilled water with a maximum injection pressure of 70 MPa and a maximum injection rate of 30 mL/min.

2.4. Experimental schemes

Fracturing tests are carried out in accordance with the experimental scheme shown in Table 1. The detailed fracturing procedures are generalized as follows:

- (1) CT scanning before fracturing. The well-developed discontinuities such as natural fractures, cavities, and calcite veins have an obvious effect on the fracturing process. Therefore, high-energy CT scanning was performed on all specimens to identify these discontinuities. The 3D reconstruction technology was then used to clearly demonstrate the number and distribution of these discontinuities.
- (2) Specimen assembly. All specimens were first completely sealed inside the high-intensity plastic film. Sodium

- bicarbonate powder was sprinkled on the surface of the sealed specimen to further protect the device from corrosion. The specimen was placed into the true tri-axial fracturing apparatus. Then, the pressure head connected to the axial pressure cap was inserted into the prefabricated borehole and the confining pressure jacks were mounted on the side of the fracturing equipment.
- (3) *In-situ stress loading*. The vertical in-situ stress was applied along the wellbore to simulate the vertical well fracturing. To avoid unbalanced loading, a vertical stress of 5 MPa was first applied to the specimen, then the minimum and maximum horizontal stresses were sequentially increased to their design values, and finally the vertical stress was increased again to the predefined value. After completing triaxial stress loading, a delay of 30 min was used to establish the stress equilibrium.
- (4) Acid or hydraulic fracturing. For single fluid fracturing, the fluid was injected along the wellbore at a constant rate until the injection pressure no longer increased or the fracture broke through the specimen boundary. For alternating injection fracturing, the timing of the switch between two different fluids is very important. Switching between the two fluids too early or too late can result in one of the fluids not being fully utilized in the fracturing process. In this study, the switching time was approximately evaluated according the size of the specimen and the injection time of single fluid fracturing. Alternating injection fracturing was achieved by

three independent fluid storage chambers with the same pumping rate. In the whole process, the specimen was not taken out and the injection line was not removed.

- (5) CT scanning after fracturing. After fracturing, the confining pressure was unloaded, the specimen was taken out and the sodium bicarbonate powder was again sprinkled on the surface of the specimen. The specimen was then scanned by high-energy CT to analyze the fracture morphology including natural and induced fractures/cavities. The specimen was then split along the induced main fractures to observe the fracture etching characteristics.
- (6) 3D laser scanning after fracturing. After splitting the specimen, one of the main fracture surfaces connected to the wellbore was selected for 3D laser scanning analysis. The amplitude of the asperity height variation within the specified window size was used to analyze the etching pattern of the main fracture surface.

3. Results and analysis

3.1. Fracture-cavity developed carbonate rocks

Fig. 4 shows the change of injection pressure with time for fracture-cavity developed carbonate rocks. Specimens #B8 and #B6 are fractured with single guar fluid and gelled acid, respectively. For specimen #B8, the injection pressure shows a trend of rapid increase followed by a sudden drop at the early stage. The injection pressure reaches its first extreme value (11.74 MPa) at about 466 s. Although there is a significant fracturing phenomenon, the injection pressure is less than the minimum horizontal principal stress (20 MPa). This indicates that only natural fractures near the wellbore may be activated by the injected guar fluid. At approximately 777 s, the injection pressure rises again and then reaches a maximum value of 14.72 MPa. This indicates that the natural fracture continues to expand until it reaches the edge of the specimen. For specimen #B6, no significant fracturing phenomenon is observed, and the injection pressure increases slowly with fluctuations. This is attributed to the leakage and etching effect of the gelled acid along the pre-existing natural fracture connected to the open hole section of the wellbore. In comparison to specimen #B8, the lower injection pressure observed in specimen #B6 may be attributed to the reduced cementation strength of the natural fractures due to the acid-rock reaction.

Specimens #B1 and #B7 are fractured with alternating injections of two fracturing fluids. For specimens #B1 and #B7, the transition times between fluid alternations are approximately 855 and 702 s, respectively (marked with green and dark blue spheres in Fig. 4). In the first fluid injection stage, the fracture initiation pressures (i.e., the first peak) for both specimens are close, but the

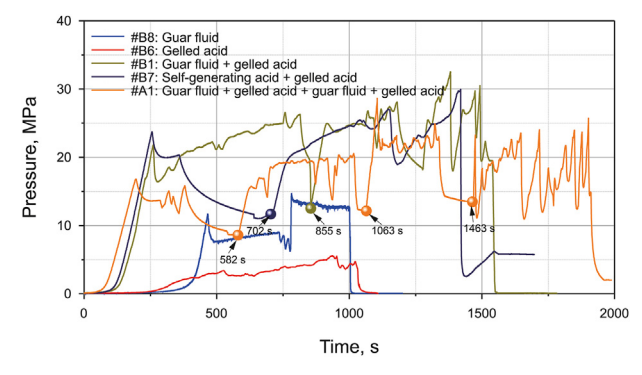


Fig. 4. Fracturing curves of fracture-cavity developed carbonate rocks.

pressure profiles following the peak pressures exhibit significant disparities. The injection pressure of specimen #B1 shows an overall upward trend except for a slight drop after the first peak, while that of specimen #B7 always shows a downward trend after the first peak. This may be attributed to differences in the type of fracturing fluids and the distribution of discontinuities. For specimen #B7, the injected self-generating acid gradually produces HCl by hydrolysis reaction, which will acidify the rock mass and reduce the fracture propagation pressure. For specimen #B1, there are no natural fractures or cavities connected to the wellbore, so a higher injection pressure is required to maintain the fracture propagation. In the second fluid injection stage, the gelled acid is used for both specimens #B1 and #B7 to further propagate the fractures and etch the fracture surfaces. The injection pressures for both specimens continue to increase with a fluctuating trend until the specimens are completely fractured.

Specimen #A1 is fractured with two alternations using guar fluid and gelled acid, where the transition times between different fluids are about 582, 1063, and 1463 s, respectively (marked with orange spheres in Fig. 4). In the first alternation (0-1063 s), the injection pressure profile for specimen #A1 is similar to that of specimen #B7, but remains below the minimum horizontal principal stress, indicating no induced artificial fractures. The primary functions of the injected guar fluid and gelled acid are to activate, unblock or etch these natural fractures around the wellbore. The etching process is further confirmed by the evident fluctuations in the fracturing curve during gelled acid injection. In the second alternation (1063–1988 s), as the guar fluid is re-pumped, the injection pressure will gradually increase and exceed the minimum horizontal principal stress. This indicates that the specimen may be fractured to form new hydraulic fractures. Finally, the injected gelled acid will flow along these open fractures and etch the surfaces of these fractures, leading to significant fluctuations in the pressure curve around 20 MPa. In general, pre-existing discontinuities, fracturing fluid types and injection schemes have significant effects on the fracture initiation and propagation. Alternating injection of different fracturing fluids is beneficial to further increasing the injection pressure and inducing the generation of new fractures.

Fig. 5 presents a comparison of the fracture morphology before and after fracturing based on 3D CT reconstruction. In addition, the etching degree of one of the fracture surfaces is characterized using 3D laser scanning analysis. Prior to fracturing, both specimens #B8 and #B6 exhibit three natural fractures, but the distribution of these natural fractures is fully different. For specimen #B8, three natural fractures are located at the bottom of the specimen, but only a natural fracture near the wellbore is activated and extended after fracturing. For specimen #B6, three natural fractures are almost perpendicular to the wellbore, and two of them intersect with the wellbore. After fracturing, the two transverse fractures are activated and extended, and some acid-etched fractures are also formed around the natural fractures due to acid erosion. Comparing specimens #B6 with #B8, fracturing with guar fluid mainly extends the existing natural fractures, while fracturing with gelled acid can generate some short acid-etched fractures. In addition, the channel etching pattern is observed in specimen #B6 adopting gelled acid as the fracturing fluid, resulting in a rougher fracture surface.

Specimen #B1 contains randomly distributed natural fractures and cavities that are located away from the wellbore. During fracturing, a tortuous fracture extends in two directions perpendicular to the minimum horizontal and vertical principal stresses, respectively. With the injection of the gelled acid, the induced fracture can connect and even partially cross the natural fracture and some cavities under the coupled hydraulic-chemical effect. The etching morphology of the tortuous fracture is heterogeneous, with higher

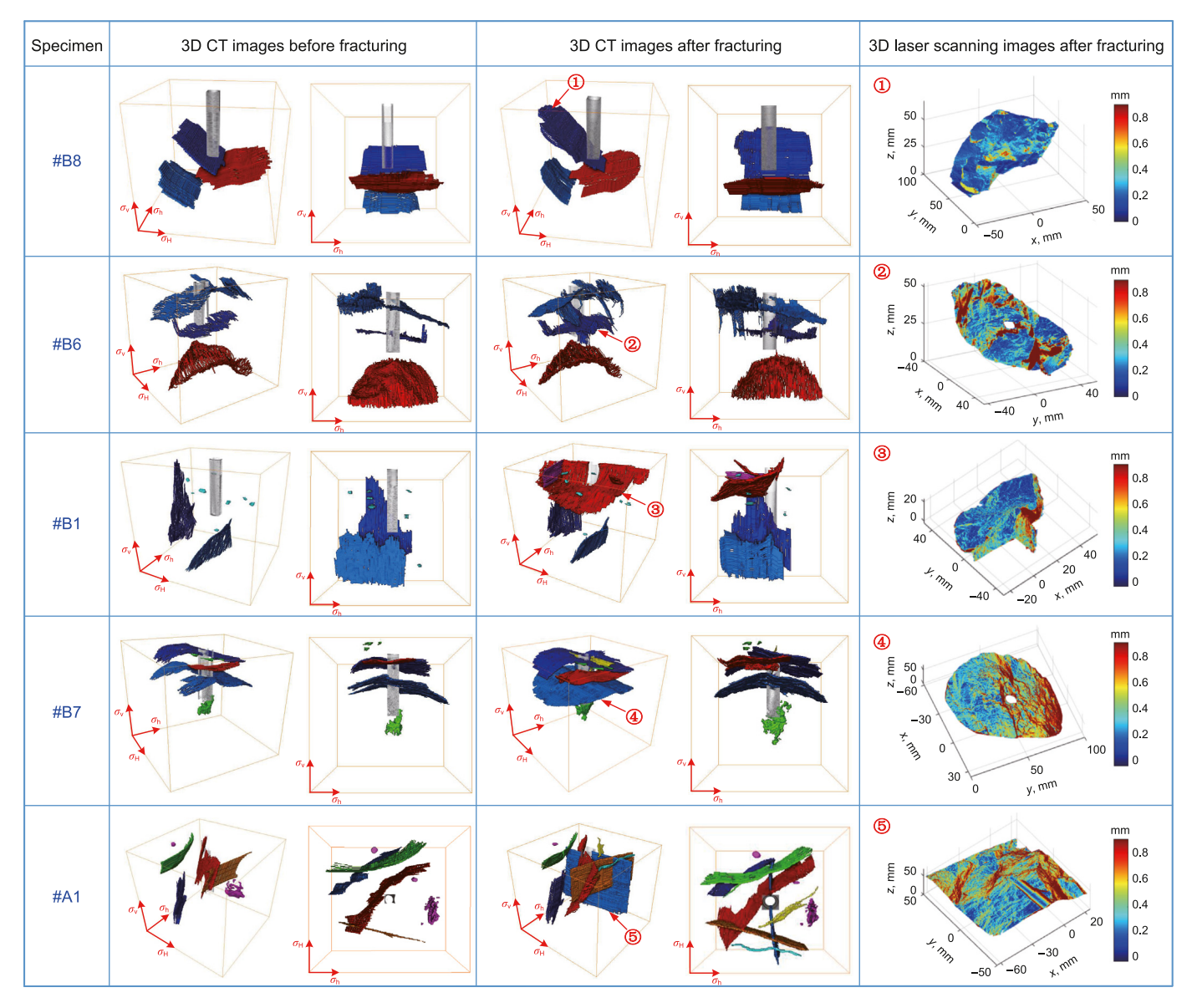


Fig. 5. Fracturing results of fracture-cavity developed carbonate rocks. The color legend in the 3D laser scanning images represents the amplitude of the asperity height variation. The greater the amplitude of the asperity height variation, the rougher the fracture surfaces, indicting a stronger etching effect.

surface roughness in the vertical fracture proximal to the wellbore. Similar to specimen #B6, specimen #B7 also has three natural fractures that are almost perpendicular to the wellbore. The difference is that in specimen #B7, all three natural fractures are connected to the wellbore and filled with calcite veins and other non-dissolved minerals. After acid fracturing, both the calcite-filled three fractures and the cavities at the bottom of the wellbore are dredged and enlarged by pressurization and dissolution. The etching pattern of the main fracture surface is also uneven, showing a higher etching degree in the right-hand zone.

Specimen #A1 contains numerous natural fractures in the vicinity of the wellbore. During the first alternation, the natural fracture connected to the wellbore is activated by the injected guar fluid and then etched by the trailing gelled acid. Although the activated natural fracture can provide the preferential flow channels, the fracturing fluid injected as the pad fluid during the first alternation can effectively prevent the leakage of the subsequent fluid. Thereafter, during the second alternation, a new hydraulic

fracture perpendicular to the minimum horizontal principal stress is generated with the re-injection of the guar fluid. The hydraulic fracture penetrates and connects with some natural fractures to form a complex fracture network. The conductivity of the interconnected fracture network is further enhanced by the etching effect of the re-injected gelled acid. Consequently, a localized channel etching pattern is observed in this specimen.

In general, it is challenging to create new artificial fractures in fracture-cavity developed carbonate reservoirs, and the final fracture morphology is primarily dominated by the distribution of natural fractures. Interestingly, alternating injection of different fracturing fluids can produce significant pressure fluctuations, which are favorable for inducing the formation of new hydraulic or acid-etched fractures. Increasing the number of the alternation injections may even create depth-penetrating hydraulic fractures. Additionally, alternating injection fracturing can expand the etching area, resulting in rougher fracture surfaces and higher hydraulic conductivity.

3.2. Fracture-cavity undeveloped carbonate rocks

Fig. 6 shows the change of injection pressure with time for fracture-cavity undeveloped carbonate rocks. These specimens are free of natural fractures and cavities, or have some natural fractures and cavities but away from the wellbore. Specimens #A4 and #A10 are fractured with single guar fluid and gelled acid, respectively. It can be seen that the changes in the injection pressure are almost consistent for both specimens. The injection pressure curve exhibits a series of sharp spikes and dips, indicating that the specimens are undergoing multiple brittle fractures. The maximum injection pressures for specimens #A4 and #A10 are 41.5 and 36.4 MPa, respectively. This indicates that the initiation pressure can be reduced through gelled acid fracturing due to rock deterioration caused by the acid-rock reaction.

Specimens #A2 and #A3 are fractured with alternating injections of two fracturing fluids. The transition times between two fracturing fluids are approximately 882 and 893 s, respectively (marked with green and dark blue spheres in Fig. 6). In the first fluid injection stage, both specimens show obvious fracturing characteristics, but specimen #A3, which is first fractured with selfgenerating acid, has a longer initiation time and a lower breakdown pressure. After the first rupture, the injection pressure of specimen #A2 increases again, while the injection pressure of specimen #A3 remains almost constant. This may be because the propagating hydraulic fracture in specimen #A2 experiences multiple ruptures or encounters some cavities. Therefore, re-pressurization is required to sustain subsequent fracture propagation or to break through these cavities. However, fracturing with self-generating acid in specimen #A3 can induce a highly conductive fracture that runs through the entire specimen. In the second fluid injection stage, the injection pressure of specimen #A2 is obviously higher than that of specimen #A3. In specimen #A2, the injected pressure decreases slowly but is always greater than 20 MPa, while the opposite trend is observed in specimen #A3. This indicates that in specimen #A2, the injected acid gradually leaks into these fractures/cavities, and then drives the fracture to propagate or break through these cavities by the pressure-coupled-dissolution effect. However, the primary role of the second fluid in specimen #A3 is to etch the main fracture surfaces. Unfortunately, no significant increase in injection pressure is observed in fracture-cavity undeveloped carbonate rocks during alternating fracturing.

Specimen #A6 is fractured with two alternations using guar fluid and gelled acid, and the diverting acid is added as a temporary plug between the two stages. The transition times between guar fluid and gelled acid are 580 and 2049 s for the first and second alternating stages, respectively, and the diverting acid is injected at intervals ranging from 1141 to 1461 s (marked with orange spheres in Fig. 6). In the first alternating stage (0–1141 s), the injection

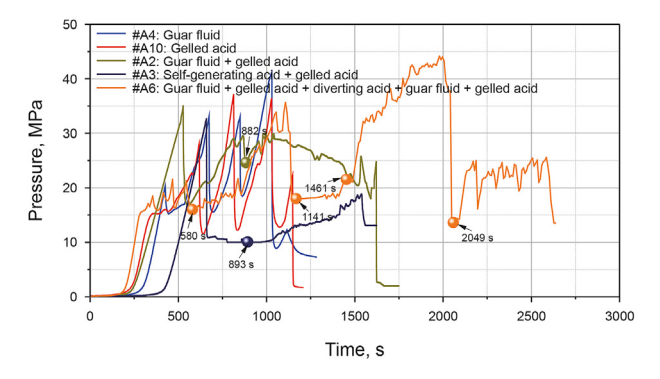


Fig. 6. Fracturing curves of fracture-cavity undeveloped carbonate rocks.

pressure gradually increases in a fluctuation form with the injection of the two fluids. The maximum injection pressure for the guar fluid is about 20 MPa, which is not inadequate to induce the hydraulic fracture. With the injection of the gelled acid, the maximum injection pressure reaches 35.64 MPa, indicating that an artificial fracture may be induced in specimen #A6. Subsequently, the diverting acid is injected at a relatively constant pressure to temporarily seal these open fractures. In the second alternating stage (1461–2628 s), as the guar fluid is re-injected, the injection pressure increases again until it reaches a maximum pressure of 52.8 MPa. This is followed by a sudden pressure drop, indicating that new hydraulic fractures may be formed. Finally, the injection pressure remains almost constant in the form of fluctuations around the minimum horizontal principal stress. This suggests that the gelled acid injected in the tail plays a major role in further etching these induced fractures. In general, the fracturing curves of all specimens exhibit obvious fracturing phenomena, indicating that different fracturing schemes can create artificial fractures in fracture-cavity undeveloped carbonate rocks. The addition of diverting acid along with the use of alternating injection fracturing can further increase the injection pressure, which is favorable for both inducing new fractures and enhancing the etching degree of the fracture.

Fig. 7 presents the fracture morphology of fracture-cavity undeveloped carbonate rocks based on 3D CT reconstruction and 3D laser scanning. It can be seen from the CT reconstruction before fracturing that there are only a few natural fractures and cavities in all the specimens, but all of them are far away from the wellbore. After fracturing, for specimens #A4, #A10, #A2, and #A3, only one artificial fracture is induced approximately perpendicular to the minimum horizontal principal stress, but the tortuosity of these fractures is different. Comparing specimens #A10 with #A4, fracturing with gelled acid can produce a more tortuous and rougher fracture due to the chemical erosion effect. Comparing specimens #A2 and #A3 with specimens #A4 and #A10, it can be seen that fracturing with alternating injection of different fluids can also induce more tortuous fractures. In addition, some cavities may be connected and even crossed by the propagating hydraulic fracture (see specimen #A2), and the acid-etched wormholes are also found in the surface of specimen #A3. For specimen #A6, three artificial fractures are finally induced, two of which are nearly vertical fractures while the other is an inclined fracture. This indicates that the addition of a temporary plugging agent (e.g., diverting acid) between two alternating stages can induce the formation of new fractures and improve the stimulation effect.

The etching degree of specimen #A10 fractured with gelled acid is evidently higher than that of specimen #A4 fractured with guar fluid. With the exception of specimen #A3, alternating injection fracturing with different fluids can form larger etching zones with greater roughness relative to single fluid fracturing. In specimen #A3, a fairly wide hydraulic fracture is formed (see Section 4.2), causing most of the subsequently injected acid to flow towards the base of the rock. The result is the formation of a higher roughness at the bottom of the fracture. In contrast to the localized etching in most fracture-cavity developed specimens, the global or regional etching pattern is observed in fracture-cavity undeveloped specimens. Overall, the etching degree of the main fracture is higher in fracture-cavity undeveloped carbonate rocks because more acid is available to react with the single fracture surface.

4. Discussion

In this part, one will further discuss the effects of the fluid type, fracture-cavity development degree, and injection schemes on the fracturing characteristics, including injection pressure, fracture

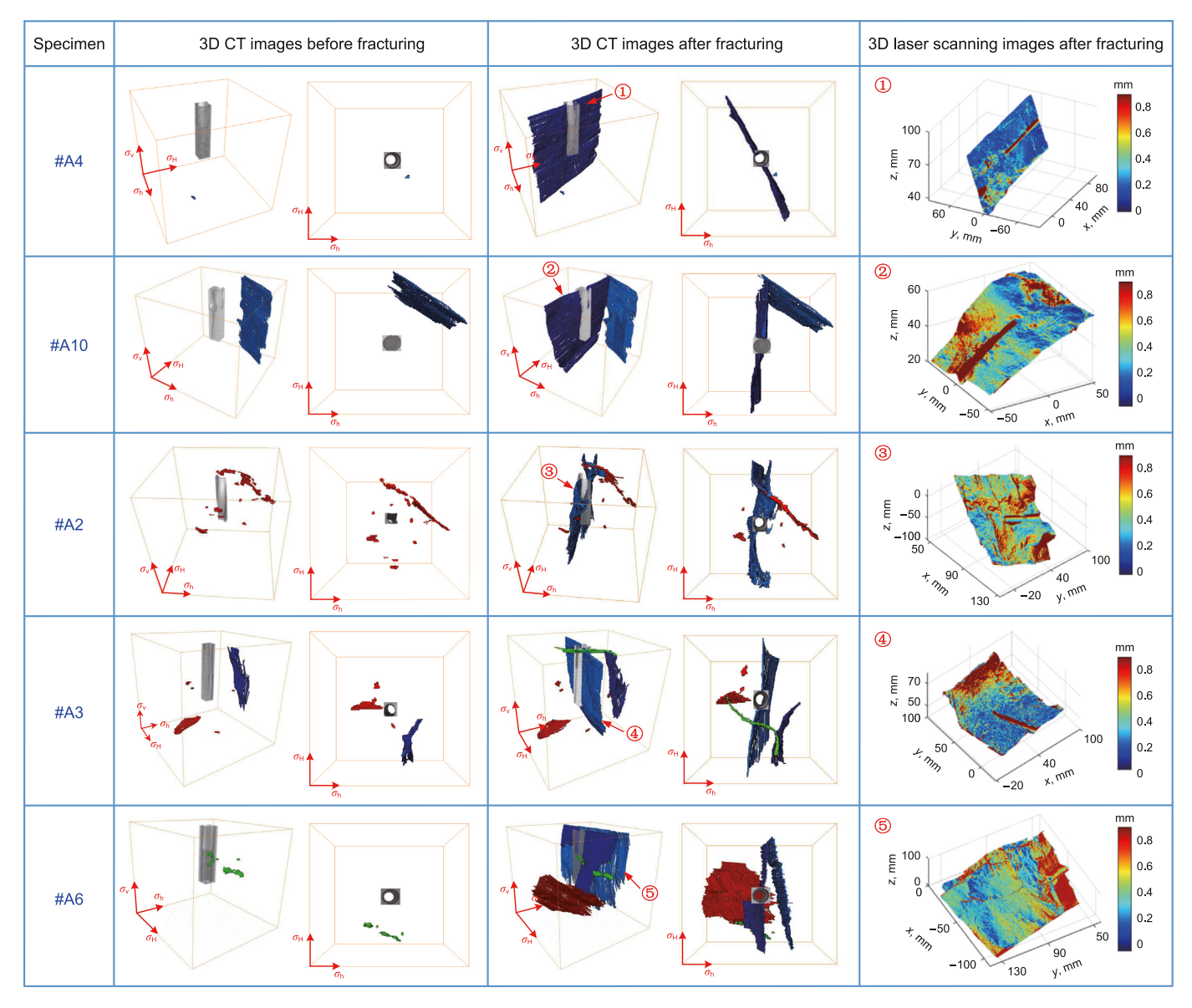


Fig. 7. Fracturing results of fracture-cavity undeveloped carbonate rocks. The color legend in the 3D laser scanning images represents the amplitude of the asperity height variation. The greater the amplitude of the asperity height variation, the rougher the fracture surfaces, indicting a stronger etching effect.

morphology, stimulation effect, and interaction behavior between induced fracture and natural fractures/cavities.

4.1. Comparison of the injection pressure for different fracturing cases

Fig. 8 depicts a comparison of injection pressures for different specimens, where the injection pressure reflects the pressure required to initiate fractures or reopen natural fractures at different injection stages. Specimens #B8 and #B6, as well as #A4 and #A10, show that fracturing with gelled acid requires lower injection pressures for both fracture-cavity developed and undeveloped carbonate rocks. Comparing specimens #B7 with #B1 or #A3 with #A2, the injection pressures for the first fluid injection are comparable; however, specimens #B7 and #A3, which are first fractured with self-generating acid, have lower injection pressures for the second fluid injection. It makes sense that although self-generating acid has a somewhat low reaction rate at the beginning of the injection, the small amount of acid generated in the later

stages can still degrade the rock. The injection pressure of fracturecavity developed carbonate rocks is typically lower than that of fracture-cavity undeveloped carbonate rocks. This is because these natural fractures around the wellbore can be easily activated or unblocked by the hydraulic-chemical coupling effect, which can provide the weak sites for fracture initiation. For fracture-cavity developed carbonate rocks (specimens #B1 and #B7), alternating injection of two fracturing fluids can further increase the injection pressure, which is beneficial to inducing new fractures. In contrast, for fracture-cavity undeveloped carbonate rocks (specimens #A2 and #A3), the high injection pressure cannot be sustained when the second fluid is injected, which indicates that the subsequently injected acid fluid mainly etches the pre-induced fractures. This may be attributed to the higher conductivity of the single fracture induced in fracture-cavity undeveloped carbonate rocks, making the fracturing fluid ineffective as a pad fluid. For specimens #A1 and #A6, the injection pressure can be further enhanced through increasing the alternating stages and applying the diverting acid, respectively.

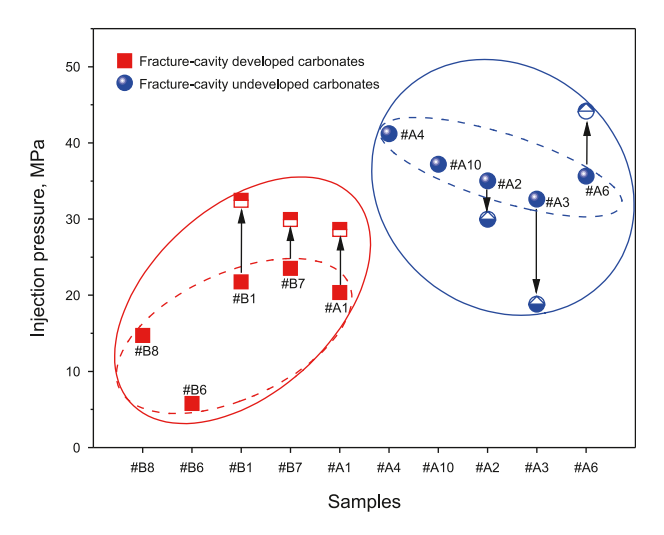


Fig. 8. Analysis of injection pressure in different carbonate rocks adopting different fracturing schemes.

4.2. Comparison of the fracture morphology for different fracturing cases

It can be found from Fig. 5 that in fracture-cavity developed carbonate rocks, the hydraulic or hydraulic-chemical coupling effect mainly acts to activate natural fractures (specimens #B8 and #A1), unblock natural fractures (specimens #B6 and #B7), or create new hydraulic fractures (specimens #B1 and #A1). Due to the leakage of the acid fluid along natural fractures, localized wormholes or etched fractures are also found in fracture-cavity developed carbonate rocks (specimens #B6 and #B7). However, in fracture-cavity undeveloped carbonate rocks, the function of the hydraulic or coupled hydraulic-chemical effect is to induce new artificial fractures (see Fig. 7). Due to the low leakage rate, the injected acid only etches the main fractures, allowing for a greater variation in the amplitude of the fracture asperity. Overall, regardless of the injection scheme, the complexity of the induced fracture is greater in fracture-cavity developed carbonate rocks, but the roughness of the main fracture is greater in most fracture-cavity undeveloped carbonate rocks. In fracture-cavity developed carbonate rocks, a complex fracture network consisting of hydraulic fractures, acid-etched fractures/wormholes, and activated natural fractures will be formed after fracturing. In fracture-cavity undeveloped carbonate rocks, with the exception of specimen #A2, a single vertical or tortuous fracture is formed after fracturing. The differences in fracture morphology for different specimens will be further discussed by the representative 2D CT scanning images, as shown in Figs. 9 and 10.

Comparing specimens #B8 with #B6 or #A4 with #A10, it is clear that fracturing with gelled acid can induce fractures with greater width due to the etching effect, and the fracture width decreases progressively with the distance away from the wellbore. Comparing specimens #B1 with #B8 (or #B6) or specimens #A2 with #A4 (or #A10), fracturing with alternating injection of two fluids can generate more complex fracture morphology. Different types of fractures, such as hydraulic fractures, acid-etched fractures and wormholes, as well as the interaction modes between induced fracture and natural fractures/cavities (see Section 4.4) are observed during alternating fracturing. This is because the alternating injection of two fracturing fluids can give full play to the role of the guar fluid in creating fractures and the gelled acid in etching

fractures. Comparing specimens #B7 with #B1 or specimens #A3 with #A2, the stimulation effect is comparable. The reason for this is that the self-generating acid with a low reaction rate at room temperature has the same pressure-induced fracture function as the guar fluid. However, the final fracture width is still larger in these specimens fractured with self-generating acid as the first fluid. This indicates that the self-generating acid also has the ability to improve the conductivity of the fractures even at relatively low acid-rock reaction rates.

Comparing specimens #A1 with #B1, it can be found that increasing the number of the alternating stages is favorable for inducing depth-penetrating fractures that can break through these natural fractures around the wellbore. This can be attributed to the fact that the pre-injected fluid, which acts as a pad fluid to form a viscous barrier, has the ability to reduce the subsequent fluid loss. Moreover, the injected gelled acid has the ability to deteriorate the fracture surface, which can provide the weak sites for fracture penetration. Finally, the depth-penetrating fracture can connect with some natural fractures and cavities to form a more complex fracture network. Comparing specimens #A6 and #A2, it can be seen that the addition of the diverting acid to the two alternating injection stages can induce new artificial fractures. This is because the viscosity of the diverting acid will increase as the acid-rock reaction proceeds. The high-viscosity diverting acid will act as a temporary plugging agent to prevent subsequent fluids from flowing into the pre-formed fractures.

4.3. Comparison of the stimulation effect for different fracturing cases

Fig. 11 shows a comparison of the stimulation effect of different specimens with different fracturing schemes. The stimulation effect is evaluated by the area, number and roughness of the fractures. where the roughness is evaluated by the arithmetic mean deviation of the height variation of the fracture surface based on 3D laser scanning. As a whole, the fracturing effect is dominated by the degree of development of natural fractures and cavities. The number and area of the fractures in fracture-cavity developed carbonate rocks are generally superior to those in fracture-cavity undeveloped carbonate rocks. However, the roughness of the main fracture is higher in most fracture-cavity undeveloped carbonate rocks. The reason for this is that the injected acid reacts primarily with the single fracture surface. In fracture-cavity developed carbonate rocks, the acid fluid will leak along these interconnected fractures, resulting in enhanced conductivity throughout the rock, rather than in a single fracture. Regardless of the degree of development of fractures and cavities, alternating injection fracturing is generally superior to single fluid fracturing. Relative to hydraulic fracturing, the roughness and complexity of the induced fractures are greater for acid fracturing. The stimulation effect of self-generating acid alternating with gelled acid is slightly better than that of guar fluid alternating with gelled acid. Considering the cost, a fracturing scheme with alternating injections of guar fluid and gelled acid may be preferable. For fracture-cavity undeveloped carbonate rocks, it is recommended to increase the number of alternating stages in conjunction with the temporary plugging technology to induce more artificial fractures. For fracture-cavity developed carbonate rocks, it is recommended to increase the number of alternating stages to generate depthpenetrating fractures, which has the advantage of connecting more natural fractures and cavities. Meanwhile, the trailing acid fluid during multiple alternating injections also has the potential to improve the hydraulic conductivity of these interconnected fractures.

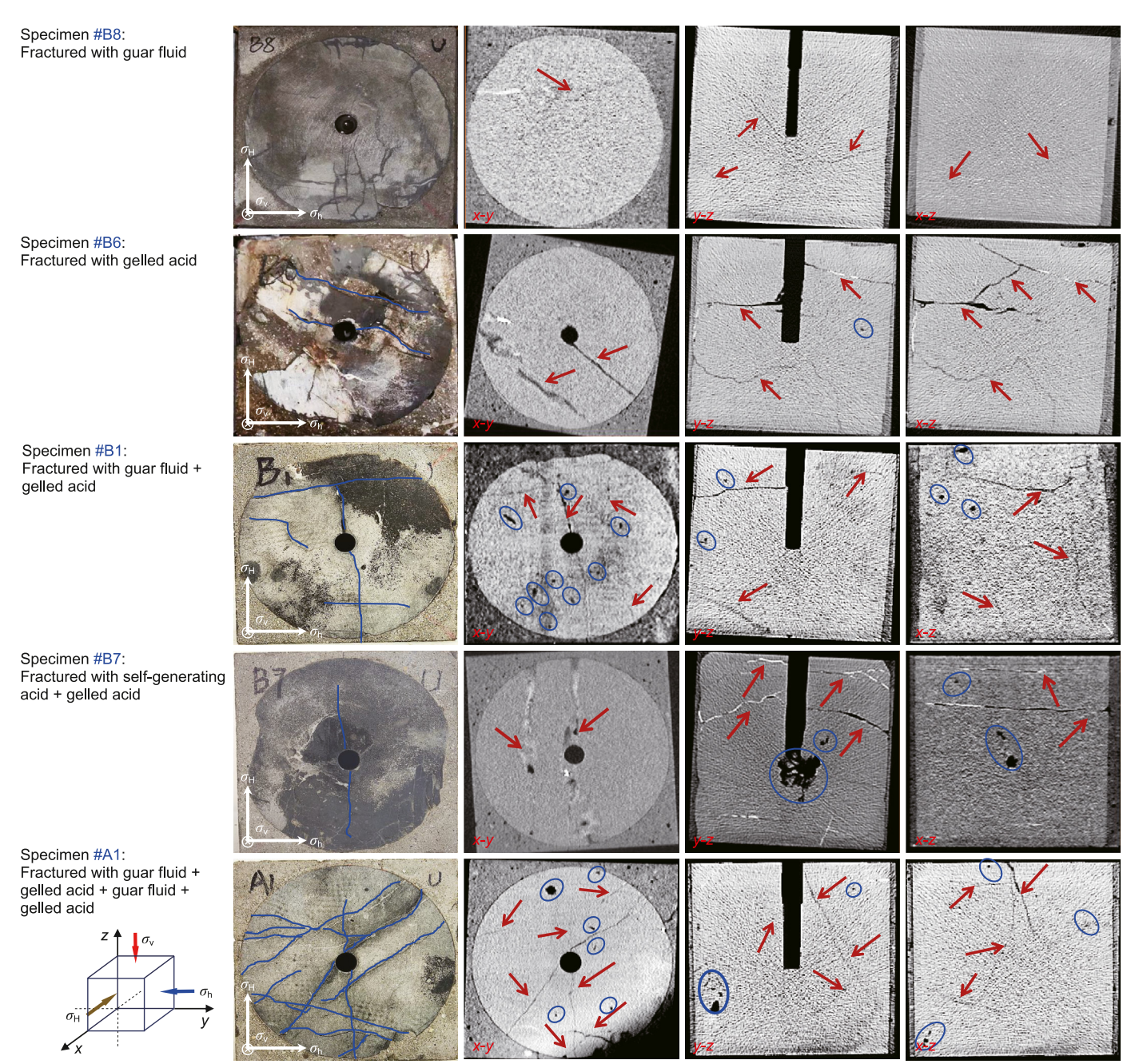


Fig. 9. Analysis of fracture propagation behavior in fracture-cavity developed carbonate rocks.

4.4. Interaction between induced fracture and natural fractures/cavities

According to Han et al. (2020), Zhang et al. (2020), and Kao et al. (2022), three propagation scenarios (crossing, deflecting/arrested, and both cases appearing) may occur when a hydraulic fracture intersects with natural fractures, while five interaction modes (crossing, bypassing, branching, arrested, killed) are possible when a fracture encounters cavities. Some interesting interaction phenomena are also observed in this study, as shown in Fig. 12. For fracture-cavity developed carbonates, most cases demonstrate that the injected fluid mainly activates and further extends pre-existing natural fractures around the wellbore, which can be regarded as the induced fracture being arrested by or deflected along these natural fractures (e.g., specimen #B6). When these natural fractures/

cavities are far away from the wellbore or undeveloped in carbonate rocks, the injected fluid can induce obvious hydraulic fractures (e.g., specimens #B1 and #A2). Theoretically, the hydraulically induced fracture will propagate perpendicular to the minimum horizontal principal stress and bypass the high stress concentration zones generated near the cavities along the way. However, during the alternating fracturing, the induced fracture may connect and even cross some fractures or cavities due to the dissolving effect of the injected acid (e.g., specimens #B1 and #A2). After crossing these natural fractures and cavities, the induced fracture will deviate from its initial propagation direction and may even bifurcate. Although some natural fractures/cavities are close to the wellbore, multistage alternating fracturing can still induce new hydraulic fractures while activating some natural fractures (e.g., specimen #A1). Under the action of the cyclic hydraulic-

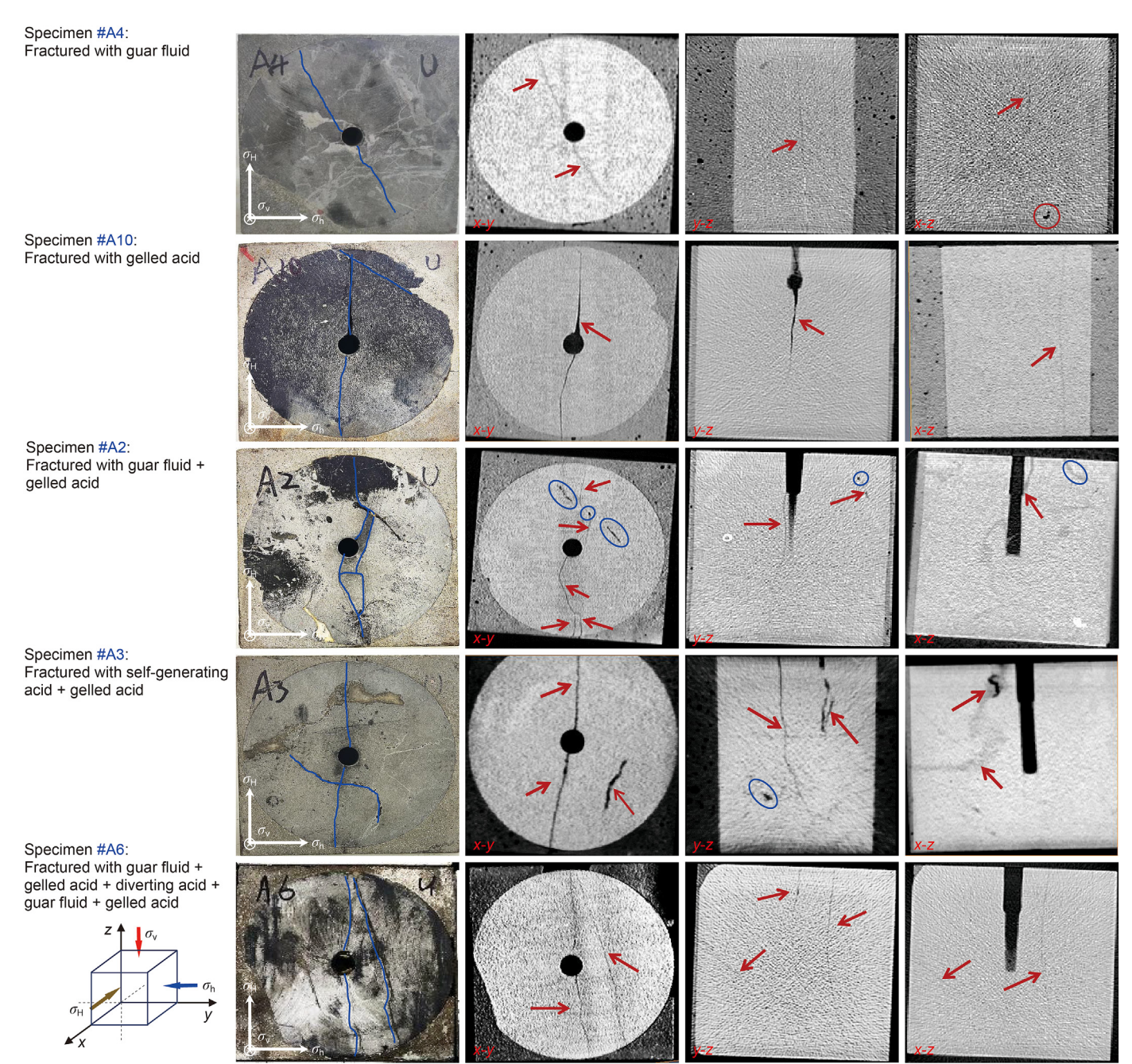


Fig. 10. Analysis of fracture propagation behavior in fracture-cavity undeveloped carbonate rocks.

chemical coupling, the induced fracture can cross or break through these natural fractures to form a depth-penetrating fracture. Unfortunately, due to the limitation of the specimen size and the randomness of the cavity, the bypassing and killed phenomena are not very obvious in this study.

5. Conclusions

To elucidate the fracturing behavior of fracture-cavity developed and undeveloped carbonate rocks, this paper uses the true triaxial fracturing experiments combined with 3D CT scanning and 3D laser scanning to investigate the effects of the fluid type, injection scheme, and fracture-cavity development on the fracturing characteristics. The meaningful conclusions are summarized as follows:

(1) Injection-induced fracturing phenomena occur in all fracture-cavity undeveloped carbonate rocks but not in fracture-cavity developed carbonate rocks. The injection pressure of fracture-cavity developed carbonate rocks is lower than that of fracture-cavity undeveloped carbonate rocks. In fracture-cavity developed carbonate rocks, alternating injection of two fluids can cause considerable pressure fluctuations and sustain relatively high injection pressures; however, this is not the case in fracture-cavity undeveloped carbonate rocks. For fracture-cavity developed and undeveloped carbonate rocks, increasing the alternating stages and employing the diverting acid can further increase the injection pressure, respectively.

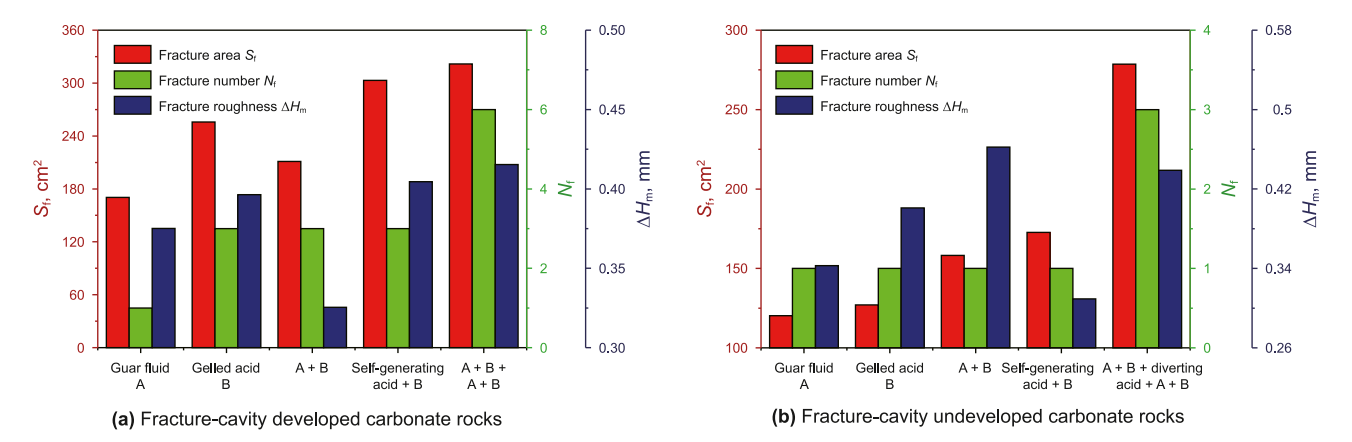


Fig. 11. Stimulation effects of carbonate rocks under different injection schemes. $N_{\rm f}$ represents the number of fractures including induced artificial fractures and activated natural fractures; $S_{\rm f}$ represents the total area of fractures including induced artificial fractures and activated natural fractures; and $\Delta H_{\rm m}$ represents the fracture roughness evaluated by the arithmetic mean deviation of the height variation of one main fracture.

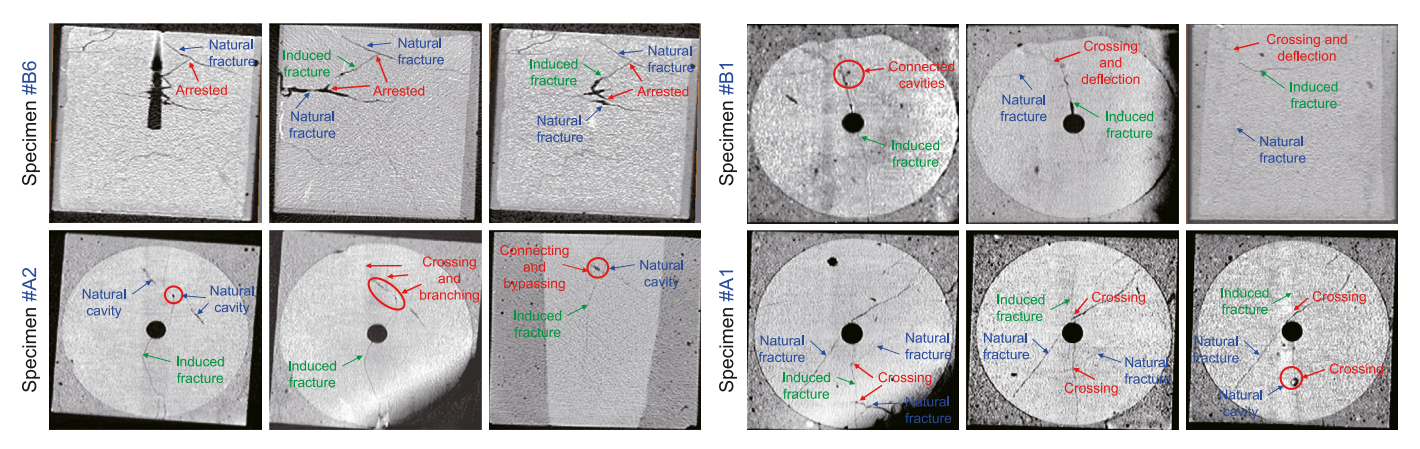


Fig. 12. Existing interaction patterns between induced fractures and natural fractures/cavities.

- (2) In fracture-cavity developed carbonate rocks, the coupled hydraulic-chemical effects serve to activate or dredge natural fractures, induce wormholes, and create acid-etched or hydraulic fractures. In contrast, their primary role in relatively homogeneous carbonate rocks is to create new hydraulic fractures. Regardless of the injection schemes, in fracturecavity carbonate rocks, the complexity of the induced fractures is usually higher, but the etching degree of the main fracture is lower due to the leakage of acid fluid along these natural fractures. Localized etching occurs in most fracturecavity specimens, whereas global etching is observed in those with undeveloped fractures and cavities.
- (3) Relative to guar fluid fracturing, the roughness and complexity of the induced fractures are greater for gelled acid fracturing. During alternating injection fracturing, guar fluid and self-generating acid, which are used as the pad fluid, have comparable stimulation effects. Alternating fracturing with guar and acid fluids can connect and even cross some natural fractures or cavities. In addition, tortuous fractures accompanied by secondary acid-etched fractures or wormholes may be induced during alternating fracturing.
- (4) Increasing the number of the alternating stages is favorable for both types of carbonate rocks. For fracture-cavity developed carbonate rocks, it is recommended to increase the number of alternating stages to generate depth-penetrating

fractures. For fracture-cavity undeveloped carbonate rocks, it is advisable to increase the number of alternating stages in conjunction with the temporary plugging technology to induce more artificial fractures.

In this study, the fracturing characteristics are analyzed based on the post-experimental fracturing curves and fracture morphology. The dynamic fracturing processes in fracture-cavity carbonate rocks are still unclear under the coupled hydraulicchemical effect. Due to the randomness of the number, size and distribution of the cavities, many interaction phenomena, such as being killed and bypassing, are not observed in this study, resulting in ambiguity regarding the interaction mechanism between induced fractures and cavities. In addition, some significant influencing factors such as acid concentration, acid dosage, temperature condition, and injection rate are not considered in this study. The number of stages for alternating acid fracturing could not be optimized due to the limitation of the specimen size. In the future, realtime monitoring of acid fracturing experiments using the acoustic emission and digital image correlation technology is needed to further reveal the dynamic fracturing behavior and interaction mechanisms. Besides, considering the challenges of experimental conditions, numerical simulations involving hydraulic-mechanicalchemical coupling effects as well as fracture-cavity interactions are also important methods to analyze the acid fracturing process.

CRediT authorship contribution statement

Song-Cai Han: Writing — original draft, Funding acquisition, Conceptualization. **Li-Le Li:** Methodology, Investigation. **Sen Hu:** Visualization, Data curation. **Chu-Hao Jing:** Validation, Formal analysis. **Xu-Di Wu:** Visualization, Investigation. **Jun-Chao Yang:** Visualization. **Tao Liu:** Supervision, Resources, Conceptualization. **Cai-Yun Xiao:** Writing — review & editing, Supervision.

Declaration of competing interest

The authors declare that they have no known competing financial interests or personal relationships that could have appeared to influence the work reported in this paper.

Acknowledgements

This study was supported by the National Natural Science Foundation of China (Grant No. 52404020 and Grant No. U1762216).

References

- Aljawad, M.S., Aljulaih, H., Mahmoud, M., et al., 2019. Integration of field, laboratory, and modeling aspects of acid fracturing: a comprehensive review. J. Petrol. Sci. Eng. 181, 106158. https://doi.org/10.1016/j.petrol.2019.06.022.
- Al-Shargabi, M., Davoodi, S., Wood, D.A., et al., 2023. A critical review of self-diverting acid treatments applied to carbonate oil and gas reservoirs. Pet. Sci. 20, 922–950. https://doi.org/10.1016/j.petsci.2022.10.005.
- 20, 922–950. https://doi.org/10.1016/j.petsci.2022.10.005.
 Chen, Y., Ma, G.W., Li, T., et al., 2018. Simulation of wormhole propagation in fractured carbonate rocks with unified pipe-network method. Comput. Geotech. 98, 58–68. https://doi.org/10.1016/j.compgeo.2017.11.009.
- Cheng, W., Jin, Y., Chen, M., et al., 2014. A criterion for identifying hydraulic fractures crossing natural fractures in 3D space. Petrol. Explor. Dev. 41 (3), 371–376. https://doi.org/10.1016/S1876-3804(14)60042-2.
- Gao, Z.B., Dai, C.L., Sun, X., et al., 2019. Investigation of cellulose nanofiber enhanced viscoelastic fracturing fluid system: increasing viscoelasticity and reducing filtration. Colloids Surf., A 582, 123938. https://doi.org/10.1016/ i.colsurfa.2019.123938.
- Gou, B., Guan, C.C., Li, X., et al., 2021. Acid-etching fracture morphology and conductivity for alternate stages of self-generating acid and gelled acid during acid-fracturing. J. Petrol. Sci. Eng. 200, 108358. https://doi.org/10.1016/j.petrol.2021.108358.
- Han, S.C., Cheng, Y.F., Gao, Q., et al., 2020. Analysis of instability mechanisms of natural fractures during the approach of a hydraulic fracture. J. Petrol. Sci. Eng. 185, 106631. https://doi.org/10.1016/j.petrol.2019.106631.
- Hou, B., Zhang, R.X., Chen, M., et al., 2019. Investigation on acid fracturing treatment in limestone formation based on true tri-axial experiment. Fuel 235, 473—484. https://doi.org/10.1016/j.fuel.2018.08.057.
- Huang, L.K., Liu, J.J., Zhang, F.S., et al., 2019. Exploring the influence of rock inherent heterogeneity and grain size on hydraulic fracturing using discrete element modeling. Int. J. Solid Struct. 176, 207–220. https://doi.org/10.1016/ j.ijsolstr.2019.06.018.
- Kao, J.W., Jin, Y., Zhang, K.P., et al., 2019. Experimental investigation on the characteristics of acid-etched fractures in acid fracturing by an improved true triaxial equipment. J. Petrol. Sci. Eng. 184, 106471. https://doi.org/10.1016/j.petrol.2019.106471.
- Kao, J.W., Wei, S.M., Wang, W.Z., et al., 2022. Numerical analysis of the hydraulic fracture communication modes in fracture-cavity reservoirs. Pet. Sci. 19 (5), 2227–2239. https://doi.org/10.1016/j.petsci.2022.05.011.
- Li, Y., Kang, Z.J., Xue, Z.J., et al., 2018. Theories and practices of carbonate reservoirs development in China. Petrol. Explor. Dev. 45 (4), 712–722. https://doi.org/

- 10.1016/S1876-3804(18)30074-0.
- Liu, G.H., Pang, F., Chen, Z.X., 2000. Similarity criterion in hydraulic fracturing simulation experiment. J. China. Univ. Pet., Ed. Nat. Sci. 24 (5), 45–48. https:// doi.org/10.3321/j.issn:1000-5870.2000.05.013 (in Chinese).
- Liu, J.Y., Ren, D.F., Feng, S.B., et al., 2024. Effect of acid-injection mode on conductivity for acid-fracturing stimulation in ultra-deep tight carbonate reservoirs. Processes 12 (4), 651. https://doi.org/10.3390/pr12040651.
- Liu, P.Y., Yao, J., Couples, G.D., et al., 2017. Modeling and simulation of wormhole formation during acidization of fractured carbonate rocks. J. Petrol. Sci. Eng. 154, 284–301. https://doi.org/10.1016/j.petrol.2017.04.040.
- Liu, Z.Y., Tang, X.H., Tao, S., et al., 2020. Mechanism of connecting natural caves and wells through hydraulic fracturing in fracture-cavity reservoirs. Rock Mech. Rock Eng. 53, 5511–5530. https://doi.org/10.1007/s00603-020-02225-w.
- Luo, Z.F., Zhang, N.L., Zhao, L.Q., et al., 2020. An extended finite element method for the prediction of acid-etched fracture propagation behavior in fractured-vuggy carbonate reservoirs. J. Petrol. Sci. Eng. 191, 107170. https://doi.org/10.1016/ i.netrol.2020.107170
- Mahdaviara, M., Rostami, A., Helalizadeh, A., et al., 2021. Smart modeling of viscosity of viscoelastic surfactant self-diverting acids. J. Petrol. Sci. Eng. 196, 107617. https://doi.org/10.1016/j.petrol.2020.107617.
- Mou, J.Y., Zhang, S.C., 2015. Modeling acid leakoff during multistage alternate injection of pad and acid in acid fracturing. J. Nat. Gas Sci. Eng. 26, 1161–1173. https://doi.org/10.1016/j.jngse.2015.08.007.
- Oeth, C.V., Hill, A.D., Zhu, D., et al., 2013. Characterization of small scale heterogeneity to predict acid fracture performance. J. Petrol. Sci. Eng. 110, 139–148. https://doi.org/10.1016/j.petrol.2013.08.001.
- Qiao, J.M., Tang, X.H., Hu, M.S., et al., 2022. The hydraulic fracturing with multiple influencing factors in carbonate fracture-cavity reservoirs. Comput. Geotech. 147, 104773. https://doi.org/10.1016/j.compgeo.2022.104773.
- Sarmadivaleh, M., Rasouli, V., 2015. Test design and sample preparation procedure for experimental investigation of hydraulic fracturing interaction modes. Rock Mech. Rock Eng. 48, 93–105. https://doi.org/10.1007/s00603-013-0543-z.
- Suo, Y., Zhao, Y.J., Fu, X.F., et al., 2024. Study on fracture propagation behavior of deep high-temperature shale gas based on the modified MERR criterion. Theor. Appl. Fract. Mech. 131, 104352. https://doi.org/10.1016/j.tafmec.2024.104352.
- Wang, Q., Zhou, F.J., Su, H., et al., 2024. Experimental evaluations of nano high-viscosity friction reducers to improve acid fracturing efficiency in low-permeability carbonate reservoirs. Chem. Eng. J. 483, 149358. https://doi.org/10.1016/j.cej.2024.149358.
- Wang, Y., Yang, J., Wang, T.Y., et al., 2022. Visualization experiment of multi-stage alternating injection acid fracturing. Energy Rep. 8, 9094–9103. https:// doi.org/10.1016/j.egyr.2022.07.031.
- Xu, H.R., Cheng, J.R., Zhao, Z.H., et al., 2021. Coupled thermo-hydro-mechanical-chemical modeling on acid fracturing in carbonatite geothermal reservoirs containing a heterogeneous fracture. Renew. Energy 172, 145–157. https://doi.org/10.1016/j.renene.2021.03.023.
- Yang, H.Z., Cheng, X., Yang, C.H., et al., 2024. Visualization and characterization of experimental hydraulic fractures interacting with karst fracture-cavity distributions. J. Rock Mech. Geotech. 16, 1667–1683. https://doi.org/10.1016/j.jrmge.2023.08.010.
- Zhang, K.P., Chen, M., Zhou, C.L., et al., 2020. Study of alternating acid fracturing treatment in carbonate formation based on true tri-axial experiment. J. Petrol. Sci. Eng. 192, 107268. https://doi.org/10.1016/j.petrol.2020.107268.
- Zhao, H.F., Xiong, Y.G., Zhen, H.B., et al., 2022. Experimental investigation on the fracture propagation of three-stage acid fracturing of tight sandstone gas reservoir. J. Petrol. Sci. Eng. 211, 110143. https://doi.org/10.1016/j.petrol.2022.110143.
- Zhao, L.Q., Chen, X., Zou, H.L., et al., 2020. A review of diverting agents for reservoir stimulation. J. Petrol. Sci. Eng. 187, 106734. https://doi.org/10.1016/ j.petrol.2019.106734.
- Zhou, Z., Wang, X., Zhao, Z., et al., 2007. New formula for acid fracturing in low permeability gas reservoirs: experimental study and field application. J. Petrol. Sci. Eng. 59 (3–4), 257–262. https://doi.org/10.1016/j.petrol.2007.04.007.
- Zhu, T.C., Wei, X.C., Zhang, Z.N., 2023. Numerical simulation of hydraulic-mechanical-chemical field coupled acid fracturing in complex carbonate reservoir. Comput. Geotech. 156, 105277. https://doi.org/10.1016/j.compgeo.2023.105277.